ADVANCED BIOSYSTEMS
www.adv-biosys.com

Facile Synthesis and Characterization of a Novel Tamavidin-Luciferase Reporter Fusion Protein for Universal Signaling Applications

*David B. Broyles, Emre Dikici, Sylvia Daunert, and Sapna K. Deo**

Despite the avidin/biotin reaction being one of the most ubiquitous noncovalent immobilization and sensing strategies in scientific research, the ability to synthesize useful amounts of biotin-binding fusion constructs is hampered by poor solubility in bacterial expression systems. As such, there are few reports of successful genetic reporter fusions incorporating a biotin-binding partner. To address this, a sensitivity-enhanced, synthetically facile reporter fusion is developed to merge the bioluminescence output of *Gaussia* luciferase (Gluc) with the recently characterized biotin-binding ability of tamavidin 2 (TA2) for general and universal signaling applications in biological and analytical systems. This fusion construct enables direct bacterial expression of a reporter system incorporating two important functionalities in a 1:1 stoichiometric relationship that can provide detection of discrete events at low concentrations. Using a cold-shock expression system, highly concentrated construct can be obtained from standard culture volumes while retaining essentially native protein activity. To demonstrate feasibility and provide an example application, this fusion construct is then included in a standard target-bridged assay design for the sensitive detection of four miRNA targets.

Protein fusions are prevalent in natural systems, and with the realization that the intentional tethering of dissimilar proteins leads to both novel functionality and confinement of unique activities, the creation of synthetic fusions involving a wide array of chemical and genetic linkages has become commonplace.[1] Many examples of synthetic fusion constructs exist, with sensors and imaging agents providing a significant percentage of these designs. A common strategy for developing analytical sensors and imaging probes is the tethering of a fluorescent or luminescent protein to an immobilization domain—frequently a biotin-binding partner. This enables specific binding to a nanocarrier, resonance energy transfer partner, or surface. Although biotin-binding reporter constructs have an extremely broad range of application, it is typically difficult to develop an appropriate expression vector such that both partners are equally soluble during expression.[2] Traditionally, proteins that were difficult to express as a fusion were purified independently and then fused using chemical conjugation techniques. This is often the only recourse when the necessity of production-level synthesis does not overlap with an available bacterial expression system. While chemical conjugations are relatively simple to generate using the large variety of specialized crosslinkers available, it is often much more difficult to control the conjugation stoichiometry and generate reproducible signals at low concentrations.

This has been the case for probably the most ubiquitous immobilization proteins in current use, avidin-like proteins. These proteins provide an extremely high affinity and selective binding interaction with their small-molecule ligand biotin, and the biotin/avidin interaction remains one of the simplest methods for noncovalent linkage. Chemical fusions are common in these systems, with associated increases in purification and stoichiometric complexity as well as decreases in total yield proportional to the number of steps after expression. Although genetic fusions can be more difficult to develop and optimize initially, they result in completely reproducible stoichiometry for straightforward and sensitive quantitative analysis[3] while being available for use almost immediately following purification rather than requiring additional reactions and expensive cleanup steps that are often necessary for chemical conjugations. However, avidin-like proteins have been particularly difficult to express and purify in a bacterial system, and although there are limited reports of soluble fusion construct expression,[4] other reports still indicate challenges[5] and provide justification for the current standard of chemically fused, avidin-like protein conjugates.

To combine the general utility of a luminescent reporter/avidin-like fusion construct with the flexibility and high yields of bacterial expression, we report a novel universal reporter/imaging construct composed of the recently described[6] biotin-binding protein tamavidin 2 (TA2) and the extremely small and bright luminescent reporter *Gaussia* luciferase (Gluc) to generate the fusion protein TA2Gluc. This genetic fusion pair was chosen based on many factors, not the least of which was the previously demonstrated bacterial expression of TA2. Further, Gluc is also one of the smallest luciferases and represents a

Dr. D. B. Broyles, Dr. E. Dikici, Prof. S. Daunert, Prof. S. K. Deo
Department of Biochemistry and Molecular Biology
Miller School of Medicine
University of Miami
1011 NW 15th Street, Miami, FL 33136, USA
E-mail: SDeo@med.miami.edu

The ORCID identification number(s) for the author(s) of this article can be found under https://doi.org/10.1002/adbi.201900166.

DOI: 10.1002/adbi.201900166

good compromise between stability, luminescent output, and optimal activity using its native substrate, coelenterazine. This substrate is also relatively inexpensive compared to some proprietary substrates and has been previously shown to provide optimal signal output for Gluc.[7] Additionally, the entire fusion construct comprises only 347 amino acids with a final mass of 37.7 kD. Following identification of the best-performing expression construct, a comprehensive characterization was undertaken to verify that each fusion partner retained near-native activity, provided reproducible activity under a broad range of assay conditions, and generated little or no instability in the overall construct. As further evidence of the utility of this novel fusion construct, a solid-phase assay incorporating a target-bridged capture system was employed to detect miRNA, a highly relevant and difficult target that serves to highlight one of the many potential benefits of an easily expressible, sensitive luminescent reporter fusion incorporating an avidin-like partner.

From our own experience with Gluc, the expression construct was designed around a C-terminal, wild-type Gluc preceded by native TA2 (Genbank accession AB102785.1), both of which were subsequently codon-optimized for expression in *Escherichia coli* (**Figure 1**a). Sequences for each were cloned from their original vectors using primers that incorporated unique restrictions sites—providing a means for ligation and subsequent manipulation. In particular, a BamHI site was introduced at the 3′ end of TA2 for ligation of the assembly as well as potential modification at the intersection between domains without the necessity of reamplifying the entire construct. As no special expression or folding considerations were known for TA2, the individually ligated components were subcloned into the cold shock induction vector pCold I to mitigate known solubility issues with Gluc in standard expression systems.[8] Further, it was determined that a spacer/linker should be introduced between proteins to enhance the likelihood of overall construct solubility.[9]

The linker sequence that enabled the highest biotin-binding affinity in the first report of a tamavidin 2 fusion[10] (5X GGGGS, Table S1, Supporting Information) was initially tested as a 3′ addition to the N-terminal TA2 sequence and positioned just upstream of the internal BamHI restriction site. However, expression testing of this sequence, as well as a reverse-order construct with C-terminal TA2 placement, led to reduced or absent soluble expression (inset of Figure S1a, Supporting Information), while resuspension of the insoluble fraction demonstrated the presence of intact overexpression product (Figure S1b, Supporting Information). As a result, an iterative screening of linker variants (Table S1, Supporting Information) was performed in order to generate and optimize soluble expression. In reducing the distance between subunits while maintaining an unstructured linker region, it was deduced from the presence of a ≈19 kD protein (retained due to the N-terminal 6x-polyhistidine tag) and absence of bioluminescence activity (Figure S1, Supporting Information) in the crude lysate that truncation of the construct occurred, leading to soluble expression of TA2 alone. Therefore, unstructured linkers were abandoned completely in favor of a rigid, α-helical linker[9] that resulted in a 1032 bp insertion and provided a soluble fusion protein consisting of 347 amino acids with a calculated

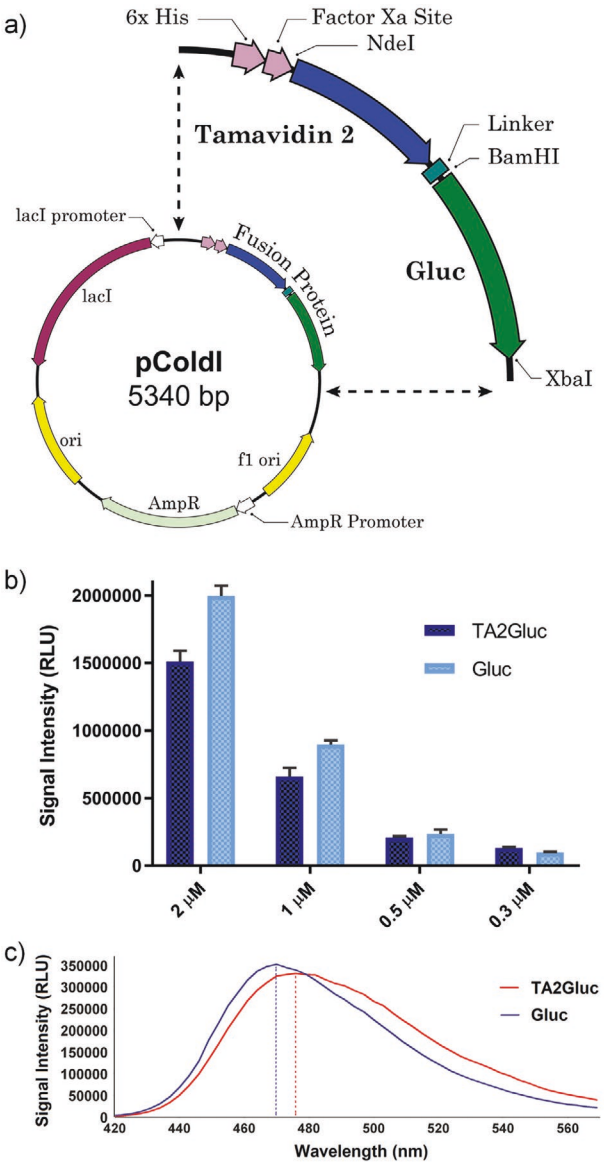

Figure 1. Construct design and preliminary activity assessment. a) Schematic representation of the pCold I host vector and insert highlighting the restriction sites, affinity tag, and orientation of the fusion partners. Total output b) of the optimal TA2Gluc construct was only minimally reduced relative to native Gluc, and c) the fusion resulted in a slightly broadened emission peak with a characteristic 6 nm red-shift.

molar mass of 37.7 kD. Although a published protocol for a different tamavidin fusion demonstrated a C-terminal fusion,[11] we discovered that an N-terminal TA2 fusion combined with a structurally rigid linker provided the optimal activity for this particular construct.

Determination of construct stability was initially assessed using total luminescent output, as measured for equimolar concentrations of fusion construct and native Gluc. Because both proteins were expressed using the pCold I expression vector under identical protocols, any differences in activity should have resulted from intrinsic effects of the fusion. From Figure 1b, bioluminescence activity of the fusion construct

averaged 79% (with a range of 74–88%) that of native Gluc over a series of twofold dilutions. Given that the crystal structure of Gluc has not yet been determined, we could only speculate as to the relative contributions of steric influence and local folding irregularities, as either or both could result in the appearance of slight inhibition. Comparative spectra (Figure 1c) provided some evidence of either a slight structural variation or vibrational energy loss, as the TA2Gluc spectrum was slightly flattened and broader than that of native Gluc and demonstrated a characteristic red-shift of exactly 6 nm (from 470 to 476 nm). Bioluminescent half-life measurements for TA2Gluc and native Gluc (Figure S2, Supporting Information) showed a similar phenomenon, with a slight increase to 5.84 s for TA2Gluc over the 5.48 s of native Gluc.

Overall structure of the construct was examined via circular dichroism (CD) spectroscopy, with contribution from TA2 compared to the known crystal structure. Conversely, the absence of X-ray or NMR structures for Gluc required comparison to literature CD structural data and structural contribution estimates.[8,12] In comparing the Gluc CD spectrum to that of TA2Gluc (**Figure 2**a), slight muting of the characteristic α-helix minima at 208 and 222 nm occurred in the TA2Gluc spectrum and may have been the result of intense β-sheet contribution from TA2 rather than being an artifact of resolution. TA2 exhibited a characteristic avidin-like CD structure,[13] and these features were evident in the TA2Gluc spectrum—especially the retention of a single global minimum centered near the inflection point of the Gluc α-helix valleys. Comparison of TA2Gluc CD spectra at 20 and 105 °C (Figure 2b) showed these valleys becoming more apparent under denaturing conditions, possibly the result of extensive disulfide formation in Gluc that allowed significant retention of secondary structure. This was also apparent during thermostability analysis under gradual denaturation, as it was impossible to observe a biphasic denaturation curve (Figure 2c). Partial attribution for the missing Gluc denaturation signal was assigned to the nonstandard observation wavelength—a necessity given that the modest change in ellipticity for Gluc at 222 nm (Figure S3, Supporting Information) was absent from the spectrum due to overwhelming contribution from the TA2 subunit of the fusion protein (Figure S4a, Supporting Information). Neither TA2Gluc nor native TA2 exhibited any change in ellipticity at 222 nm; conversely, the dominant transition for both proteins occurred at 230 nm (Figure S4a,b, Supporting Information). Some structural contribution from Gluc was evident from the reduction in melting temperature (T_m) of the fusion construct (90.74 ± 0.08 °C) when compared to native TA2 (97.39 ± 0.07 °C). Given that the independent T_m of Gluc, at 56–72 °C,[8,12] is considerably lower than that of TA2,[6] it was necessary to compare Gluc CD spectra at 20 and 105 °C (Figure S3, Supporting Information) to confirm that no significant structural change was evident following denaturation. Some stabilization of the fusion protein likely resulted from association of TA2 subunits in solution, but there was no visible evidence of a change in denaturation rate as monomeric TA2Gluc predominated.

In order to independently interrogate the structure/function relationship for each subunit, substrate binding was assessed either kinetically under ideal conditions (25 °C) or as a function of structural integrity during temperature fluctuations. For

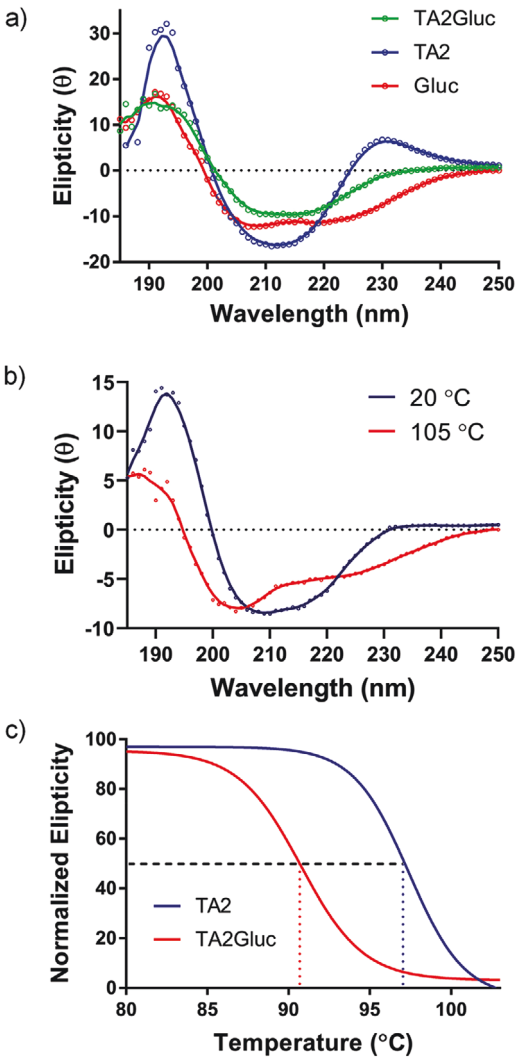

Figure 2. Structural assessment and the effect of structure on construct thermostability. a) Analysis of the circular dichroism (CD) structure of free TA2 and Gluc relative to TA2Gluc. b) Comparison of CD secondary structures for TA2Gluc before and after denaturation. c) Thermostability profile comparison for TA2 and the fusion construct.

the Gluc subunit, bioluminescence provided the most relevant activity information and was measured for equal concentrations of TA2Gluc that were heated for 10 min at a constant temperature prior to room-temperature (22 °C) measurement of bioluminescence activity. As shown in **Figure 3**a, bioluminescence output in solution dropped to approximately one-tenth of the room-temperature maximum immediately following 74 °C incubation, indicating that retention of significant secondary structure at high temperature was insufficient for maintaining biological activity. However, as is evident from Figure 3b, the application of temperature-exposed fusion protein to a biotinylated solid support only indicated a loss of approximately twofold below maximum for aliquots held at 74 °C, with a tenfold reduction not seen until 78 °C. This observation indicated that Gluc activity likely correlated with overall construct integrity, and biotin capture served to selectively concentrate the remaining active complexes. This is reinforced by the fact that

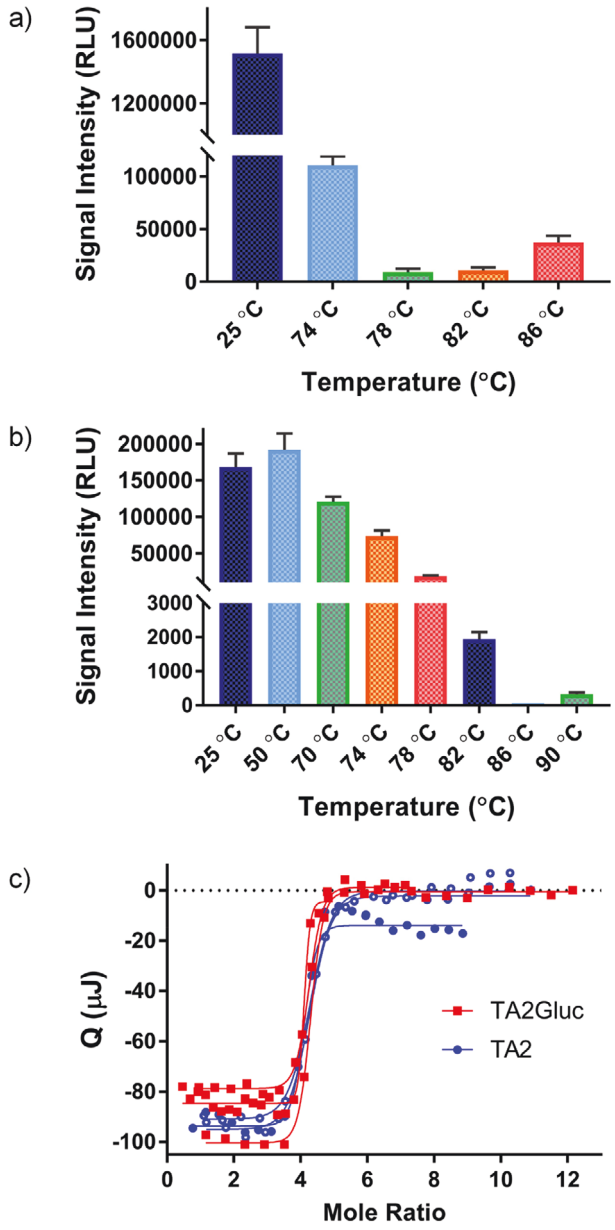

Figure 3. Substrate binding parameters for fusion construct. Bioluminescence activity of the construct was measured in a) solution-phase or b) solid-phase over a temperature range that included denaturing temperatures. c) Biotin-binding characteristics were compared between TA2Gluc and native TA2 using triplicate ITC measurements.

biotin binding occurred only after temperature exposure and could play no additional role in stabilizing the entire construct. Furthermore, essentially no change in TA2 secondary structure was observed following exposure to biotin (Figure S5, Supporting Information), indicating that any stability enhancement must have resulted from the combination of biotin binding and quaternary effects.

As opposed to TA2 alone, the fusion construct demonstrated more heterogeneity in quaternary structure (Figure S6, Supporting Information) and appeared to favor any valency beyond simple dimerization, while TA2 almost exclusively favored a tetrameric state. The effects of this discrepancy could be inferred using isothermal titration calorimetry (ITC), despite the unreliability of ITC modeling for proteins with very low dissociation constants.[14] For this, native TA2 was analyzed under identical conditions and concentration to TA2Gluc in order to provide a thermodynamic assessment of the binding environment. Figure 3c demonstrates triplicate ITC measurements for both TA2Gluc and native TA2 comparatively modeled for visual clarity using the Boltzmann sigmoid. The highly reproducible isotherms highlight the similarities between the two proteins and provide confirmation of the exceptionally high binding affinity for both. In this example, stoichiometry was adjusted to approximately whole values based on prior knowledge of available binding sites, but we also opted to display the experimental stoichiometry in Figure S7 in the Supporting Information as a comparison to the observed valency seen electrophoretically in Figure S6 in the Supporting Information. Besides stoichiometry, ITC can provide reliable estimates of enthalpy changes, and while no enthalpy data for TA2 could be located in the literature, the experimental enthalpies of -118.7 ± 3.0 and -94.4 ± 8.6 kJ mol^{-1} (Table S2, Supporting Information) for native TA2 and TA2Gluc, respectively, align closely with literature values derived for avidin and streptavidin.[15] As each TA2 subunit only binds a single biotin internally, this would seem to confirm observations by others[6] that biotin binding serves to stabilize the tetrameric state, and the slight decline in enthalpy for TA2Gluc likely reflects differences in quaternary structure. In-depth characterization of avidin/streptavidin–biotin interaction kinetics support this observation,[15,16] and although not all features of avidin-like proteins are interchangeable, mutational interruption of streptavidin tetramerization has also demonstrated a significant decrease in association constant, indicating that the independent binding pockets of each subunit are likely not in an ideal conformation prior to tetramerization.[16a–c] As such, any steric considerations that limit tetrameric association should reduce biotin-binding affinity, depress the association constant, and decrease overall thermostability. This likely correlates with the loss of secondary structure contribution from TA2 in the fusion when measured at 105 °C as well as the slight decrease in fusion thermostability (Figure 2c).

Although reporter stability is an important metric for assessing general utility, other factors that can influence design considerations are only apparent following transition to a "real-world" application. For this, an example assay system that is commonly used for short nucleic acid target detection was used to demonstrate the sensitivity of TA2Gluc as a universal reporter of target hybridization. In this "target-bridged" assay (**Figure 4**a), miRNA target serves to immobilize a reporter strand containing a terminal biotin such that the presence of target leads to a dose-dependent capture of TA2Gluc. This provided a luminescent signal equivalent to the amount of immobilized fusion construct upon addition of coelenterazine substrate. As direct detection of miRNA targets requires profound sensitivity, the signal-to-noise (S/N) ratio of the construct was optimized without consideration of dynamic range in order to observe the effect of assay stringency on detection limits. S/N calculations were performed for each analytical signal and were based on the calculation $S/N = \bar{x}/s$, where $\bar{x}$ is the average

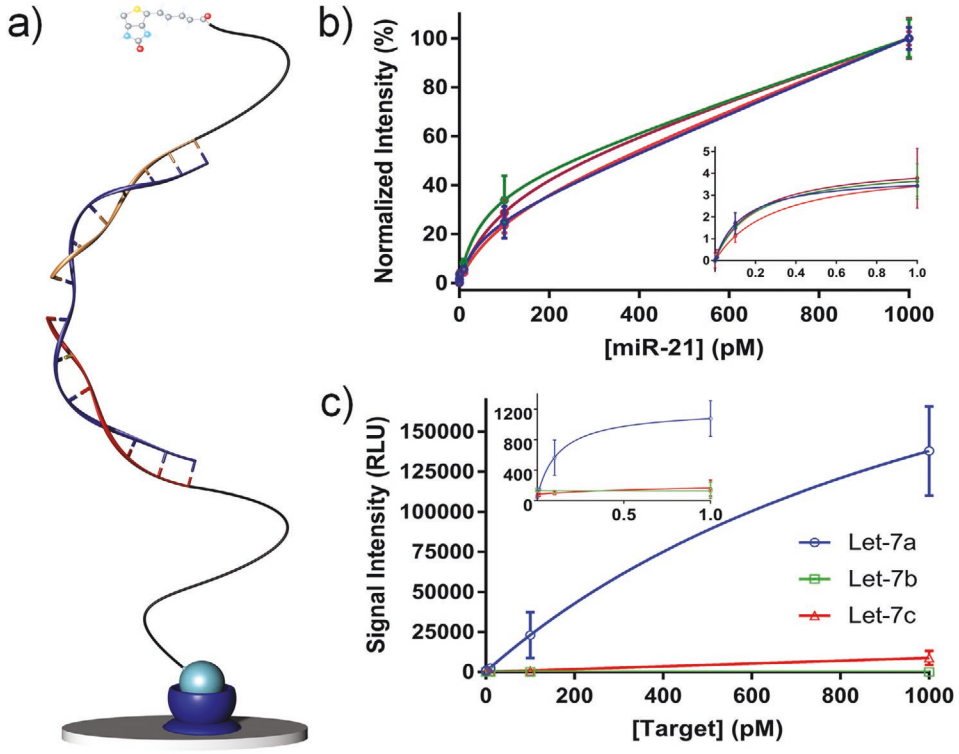

Figure 4. Assay design and performance. a) A bridged capture format and terminal biotin served to immobilize the reporter system. b) Reproducibility of standard curves for this design was demonstrated using miR-21 as a representative target at six standard calibration concentrations covering six orders of magnitude (from 1×10^{-14} to 1×10^{-9} M), and the inset shows the lower concentrations that are obscured in the main plot. Each independent run was normalized internally to the highest and lowest values within that set. c) Mismatch selectivity was demonstrated among the Let-7 family members. The insets provide a closer view of concentrations not readily visible in the main plot areas.

signal at a particular target concentration and s is the standard deviation of the mean for that signal. On average, the lowest target concentrations produced a S/N ratio of ≈10, while higher target concentrations doubled that value. Even within these stringent conditions, a dynamic range of six orders of magnitude with high reproducibility was observed (Figure 4b), with a lowest detection limit of 5.2×10^{-14} M for miR-21 based on nonlinear calibration curve fitting using GraphPad Prism software.

To verify that assay stringency was sufficient for analytical utility, the Let-7 family of miRNA was adopted as a selectivity model due to inclusion of perfectly matched as well as 1- and 2-nucleotide mismatched targets (Figure 4c). The 1-nucleotide mismatch of Let-7c, being the most relevant analytical comparison, was found to generate an average signal of less than 6% of the perfect-matched signal. Suitability of TA2Gluc for use as a universal reporter was confirmed by employing either four individual capture/reporter systems (Figure S8, Supporting Information) or two reporter systems in crude human serum (Figure S9a,b, Supporting Information) and observing the system response under constant TA2Gluc concentration. By independently detecting each signal, an average detection limit of 2.3×10^{-13} M in buffer was achieved, with three species providing an average of less than 1.0×10^{-13} M. Surprisingly, serum had only a miniscule comparative effect on sensitivity and overall calibration performance for the miRNA tested. It was apparent, however, that each miRNA species has a distinct calibration curve that reflects the effects of individual T_m and sequence differences on equilibrium conditions, although interassay variability for unique targets, as a measure of reproducibility, was minimal.

In summary, a high degree of construct thermostability and the demonstration of appropriate sensitivity using an example miRNA detection platform provide convincing evidence of TA2Gluc utility in assay design. Besides the obvious benefits of a high-yield fusion of immobilization and reporter moieties, the time and cost savings from simplistic bacterial expression combined with excellent retention of activity in storage (>6 months at 4 °C) and the lack of postexpression manipulation translate to a robust assortment of potential applications ranging from analytical assay development to in situ tracking and imaging. Given the recent emphasis on merging in vitro imaging systems with bioluminescent tracking to provide deep-tissue penetration, this construct and its serum-stable constituents could provide a more efficient route to labeling. Likewise, advances in isothermal amplification technologies as well as portable assay designs provide many systems that could easily incorporate this construct, enabling reduced complexity and production time for point-of-care devices.[17] The sensitivity of bioluminescence, the prodigious binding affinity of biotin-binding proteins, the universal nature of biotin recognition, and the simplicity of bacterial expression make this construct uniquely valuable for modern biotechnology.

Supporting Information

Supporting Information is available from the Wiley Online Library or from the author.

Acknowledgements

The authors would like to thank NIGMS (R01GM114321 and R01GM127706) and the National Science Foundation (CHE-1506740 and CBET-1841419) for funding support. S.D. thanks the Miller School of Medicine of the University of Miami for the Lucille P. Markey Chair in Biochemistry and Molecular Biology.

Conflict of Interest

The authors declare no conflict of interest.

Keywords

bioluminescence, imaging agents, optical reporters

Received: July 29, 2019
Revised: February 6, 2020
Published online: February 28, 2020

[1] K. Yu, C. Liu, B. G. Kim, D. Y. Lee, *Biotechnol. Adv.* **2015**, *33*, 155.
[2] M. Lebendiker, T. Danieli, *FEBS Lett.* **2014**, *588*, 236.
[3] V. Grigorenko, I. Andreeva, T. Borchers, F. Spener, A. Egorov, *Anal. Chem.* **2001**, *73*, 1134.
[4] a) S. Inouye, J. Sato, S. Sasaki, Y. Sahara, *Biosci., Biotechnol., Biochem.* **2011**, *75*, 568; b) D. V. Smirnova, M. Y. Rubtsova, V. G. Grigorenko, N. N. Ugarova, *Photochem. Photobiol.* **2017**, *93*, 541.
[5] a) R. Modanloo Jouybari, A. Sadeghi, B. Khansarinejad, S. Sadoogh Abbasian, H. Abtahi, *Rep. Biochem. Mol. Biol.* **2018**, *6*, 178; b) L. Arribillaga, M. Durantez, T. Lozano, F. Rudilla, F. Rehberger, N. Casares, L. Villanueva, M. Martinez, M. Gorraiz, F. Borras-Cuesta, P. Sarobe, J. Prieto, J. J. Lasarte, *BioMed Res. Int.* **2013**, *2013*, 864720.
[6] Y. Takakura, M. Tsunashima, J. Suzuki, S. Usami, Y. Kakuta, N. Okino, M. Ito, T. Yamamoto, *FEBS J.* **2009**, *276*, 1383.
[7] T. Kimura, K. Hiraoka, N. Kasahara, C. R. Logg, *J. Gene Med.* **2010**, *12*, 528.
[8] T. Rathnayaka, M. Tawa, S. Sohya, M. Yohda, Y. Kuroda, *Biochim. Biophys. Acta, Proteins Proteomics* **2010**, *1804*, 1902.
[9] X. Chen, J. L. Zaro, W. C. Shen, *Adv. Drug Delivery Rev.* **2013**, *65*, 1357.
[10] Y. Takakura, N. Oka, H. Kajiwara, M. Tsunashima, S. Usami, H. Tsukamoto, Y. Ishida, T. Yamamoto, *J. Biotechnol.* **2010**, *145*, 317.
[11] Y. Takakura, N. Oka, M. Tsunashima, *Methods Mol. Biol.* **2014**, *1177*, 95.
[12] M. D. Larionova, S. V. Markova, E. S. Vysotski, *J. Photochem. Photobiol., B* **2018**, *183*, 309.
[13] a) R. W. Woody, *Eur. Biophys. J.* **1994**, *23*, 253; b) A. Micsonai, F. Wien, L. Kernya, Y. H. Lee, Y. Goto, M. Refregiers, J. Kardos, *Proc. Natl. Acad. Sci. USA* **2015**, *112*, E3095.
[14] J. A. Maatta, T. T. Airenne, H. R. Nordlund, J. Janis, T. A. Paldanius, P. Vainiotalo, M. S. Johnson, M. S. Kulomaa, V. P. Hytonen, *ChemBioChem* **2008**, *9*, 1124.
[15] R. F. Delgadillo, T. C. Mueser, K. Zaleta-Rivera, K. A. Carnes, J. Gonzalez-Valdez, L. J. Parkhurst, *PLoS One* **2019**, *14*, 0204194.
[16] a) T. Sano, S. Vajda, C. L. Smith, C. R. Cantor, *Proc. Natl. Acad. Sci. USA* **1997**, *94*, 6153; b) O. H. Laitinen, H. R. Nordlund, V. P. Hytonen, S. T. Uotila, A. T. Marttila, J. Savolainen, K. J. Airenne, O. Livnah, E. A. Bayer, M. Wilchek, M. S. Kulomaa, *J. Biol. Chem.* **2003**, *278*, 4010; c) G. V. Dubacheva, C. Araya-Callis, A. Geert Volbeda, M. Fairhead, J. Codee, M. Howarth, R. P. Richter, *J. Am. Chem. Soc.* **2017**, *139*, 4157; d) N. M. Green, *Biochem. J.* **1966**, *101*, 774.
[17] R. Ramji, C. F. Cheong, H. Hirata, A. R. Rahman, C. T. Lim, *Small* **2015**, *11*, 943.

